Food Research International 157 (2022) 111292

Contents lists available at ScienceDirect

Food Research International

journal homepage: www.elsevier.com/locate/foodres

In situ SAXS study of non-fat milk model systems during heat treatment and acidification

Ruifen Li [a,*], Tanja Christine Jæger [b], Tijs A.M. Rovers [c], Birte Svensson [d], Richard Ipsen [a], Jacob J.K. Kirkensgaard [a,e], Anni Bygvrå Hougaard [a]

[a] Department of Food Science, University of Copenhagen, Rolighedsvej 26, DK-1958 Frederiksberg C, Denmark
[b] Arla Foods Ingredients Group P/S, Sønderupvej 26, DK-6920 Videbæk, Denmark
[c] Arla Foods a.m.b.a, Agro Food Park 19, 8200 Aarhus, Denmark
[d] Enzyme and Protein Chemistry, Department of Biotechnology and Biomedicine, Technical University of Denmark, Søltofts Plads, Building 224, DK-2800 Kgs. Lyngby, Denmark
[e] Niels Bohr Institute, Universitetsparken 5, 2100 København Ø, Denmark

ARTICLE INFO

Keywords:
Small-angle X-ray scattering
Casein micelle
Nano-particulated whey protein
Whey protein concentrate
Acidified gel
Interactions of milk proteins

ABSTRACT

Small-angle X-ray scattering (SAXS) was used to monitor structural changes induced by heat treatment and acid gelation in milk matrices with added whey protein concentrates (WPCs) and nano-particulated whey protein (NWP). In general, heat treatment was found to mainly affect whey protein components while pure casein micelles remained largely unaffected. Conversely, acidification mainly affected caseins while leaving pure whey protein components intact. In mixed systems, the overall behaviour could be understood as a combination of the above effects, however, the type of the added whey protein components influenced the resulting structure formation and dynamics. NWP led to formation of larger structures compared to WPC components during heat treatment, although the latter showed faster aggregation dynamics. During acidification the NWP containing samples exhibited structural changes at slightly higher pH values than the WPC samples. The modeling of pure liquid whey protein (LWPC) samples showed that the heat induced denaturation and resulting aggregation of individual whey proteins is mainly a surface effect leaving the overall protein shape and dimensions unaffected. Schematic diagrams based on the current SAXS data and previous studies were constructed to illustrate the suggested interaction mechanisms between casein and whey proteins during both heating and acidification.

1. Introduction

The addition of whey protein ingredients to dairy products has become a common practice as they can provide favorable nutritional and functional properties, such as increased creaminess and viscosity (Janhoj, Petersen, Frost, & Ipsen, 2006; Torres, Janhøj, Mikkelsen, & Ipsen, 2011), or softer texture (Tamime, Kalab, Muir, & Barrantes, 1995) especially in low-fat yoghurt. Heat treatment/pasteurization and acidification are integral parts of industrial processing of yogurt. In general, heat treatment will cause denaturation of whey proteins leading to partial aggregation as well as interactions with the casein micelles, and the process of acidification can lead to considerable modifications in the milk components and especially change the structure of casein micelles (Gonzalez-Jordan, Thomar, Nicolai, & Dittmer, 2015). The presence of whey protein aggregates in heated milk, both in solution and on the surface of casein micelles, then affects how acid gelation proceeds by attaching to the micelles and facilitating protein network formation (Lucey, 2002; Vasbinder, Alting, & de Kruif, 2003).

Small angle X-ray scattering (SAXS) is a non-invasive technique, which can be applied in situ for investigation of nano- and microstructures ranging from ca. 1 to 200 nm in dimensions and probe the sample in its original intact and turbid state. SAXS has been applied extensively on complex dairy matrices to understand the structure of casein micelles, which contribute to the major physicochemical and organoleptic properties in skim milk (Day et al., 2017; Ingham et al., 2016). Besides, the casein micelle can be regarded as a highly dynamic system, where an equilibrium is maintained with the surrounding serum phase in regard to inorganic components (e.g. calcium and phosphate). This protein is more susceptible to pH (Le Graët & Gaucheron 1999), temperatures (Anema & Klostermeyer, 1997), and ionic concentration (Holt, Davies,

* Corresponding author.
E-mail address: ruifen.li@food.ku.dk (R. Li).

https://doi.org/10.1016/j.foodres.2022.111292
Received 3 February 2022; Received in revised form 20 April 2022; Accepted 21 April 2022
Available online 26 April 2022

& Law, 1986). The interpretation of milk scattering data has been a subject of controversy for decades, but in general, three principal domains of low-q (0.001–0.004 $Å^{-1}$), intermediate-q (0.01–0.02 $Å^{-1}$), and high-q (0.08–0.1 $Å^{-1}$) are commonly applied to SAXS data in the literature. The low-q feature indicates the form factor scattering of the moderately polydisperse casein micelles, corresponding well to micelle sizes of roughly 100–200 nm (Marchin, Putaux, Pignon, & Léonil, 2007; Mata, Udabage, & Gilbert, 2011). The intermediate-q feature is normally ascribed to the internal structure of casein micelles, representing incompressible regions of casein clusters of 10–20 nm (Ingham et al., 2016; Yang, Tyler, Ahrne, & Kirkensgaard, 2021) or 'submicelles' (Yang et al., 2018). Finally, high-q features have been argued to represent the colloidal calcium phosphate (CCP) particles and e.g. their removal from micelles as Marchin et al. (2007) found an annihilation of the high-q feature and little change at low-q, together with complete dissolving of CCP detected by cryo-transmission as pH dropped to 5.2. On the other hand, Hansen et al. (1996), using small-angle neutron scattering (SANS), ascribed high-q features to size changes of sub-micellar units when observing a similar phenomenon from pH 6.7 to 5.7. The high-q feature has also been hypothesized to be related to protein inhomogeneities on a 1–3 nm length scale, and it was argued to be unlikely to observe CCP particles with X-ray scattering as it is several orders of magnitude lower than the protein scattering (De Kruif, 2014). Ingham et al. (2016) noted that a CCP scattering feature appeared at q-values around 0.035 $Å^{-1}$ using resonant soft X-ray scattering.

The casein proteins have in recent years been reported to work as chaperones both for whey proteins and each other (He et al., 2011; Morgan et al., 2005). The casein-casein interactions could inhibit aggregation and/or facilitate folding of a particular conformation. However, using SAXS measurements to investigate structural changes occurring when different types of whey protein ingredients are added to systems containing casein has not previously been reported.

The present study was undertaken to apply SAXS for investigating the structural changes occurring between added whey protein ingredients and native milk protein components during heat treatment and acidification in non-fat milk model systems.

2. Materials and methods

2.1. Materials and sample preparation

Powdered ingredients, whey protein concentrate (WPC, 77.0% protein, 6.5% fat, 7.5% lactose) and nano-particulated whey protein (NWP, 80.0% protein, 5.3% fat, 2.0% lactose) were provided by Arla Foods Ingredients (AFI, Nr. Vium, Denmark). The composition of the ingredients is given as reported by the manufacturer. Commercial skim milk (Com SM, 0.1% fat) was produced by Arla Foods amba (Viby, Denmark) and bought directly from a local supermarket.

Liquid casein concentrate (LCC, approximately 17% casein and 2% whey protein) and liquid whey protein concentrate (LWPC, approximately 7.1% whey protein and 0.8% casein) were obtained using microfiltration (MF) and ultrafiltration (UF), respectively at pilot plant scale. Briefly, LCC was initially produced directly from commercial skim milk using MF with a pilot-scale SW25 MMS system (MMS AG Membrane Systems, Urdorf, Switzerland) equipped with 0.1 μm nominal pore diameter ceramic membrane (Lenntech, Delfgauw, the Netherlands). The production proceeded under a controlled uniform temperature of 50 °C and a pressure of 0.5 bar. Subsequently, LWPC was continually produced from the MF permeate with UF using a UF Lab-stack (Tetra Pak, Silkeborg, Denmark) fitted with GR61PP membranes (Alfa Laval, Lund, Sweden) of 20,000 Da nominal molecular mass cut-off. The obtained permeate from UF was collected and used for dilution during sample preparation. Subsequently, LCC and LWPC samples were kept at −80 °C, and permeate at −20 °C until use. More details about the production can be found in our previous papers (Li et al., 2021a; 2021b).

For thawing of samples, the same procedure was adopted as in Li et al (2021b), i.e., the frozen samples were initially kept in a refrigerator at 5 °C for 3d, and subsequently moved to a water bath and kept at 30 °C for 30 min.

2.2. Acidified milk model systems processing in lab scale

A total of 8 milk model systems were constructed using casein (LCC) and 3 different types of whey proteins (LWPC, WPC, NWP) in different ratios, including one reference (SM) mimicking the composition of commercial skim milk and which consisted of 2.8 % LCC and 0.9% LWPC. Permeate from UF was used to dilute the samples, thus mimicking the milk environment in terms of minerals and lactose. Commercial skim milk (Com SM) was included as an additional reference. Except for the two references, all milk model systems had a total protein content of 4% (w/w) with casein and whey protein in the ratio of 1:1 (see Table 1 for more details).

Each of the mixed and diluted model systems of 300 mL were first pre-stirred at 800 rpm for 30 min with a magnetic stirrer (IKA™ RET Basic Magnetic Stirrer, Fisher Scientific, Roskilde, Denmark) at room temperature. Afterwards, they were continually stirred at a speed of 600 rpm overnight in a cold room at 5 °C, using the same magnetic stirrer. Then, a pre-heat treatment (55 °C, 5 min) was performed in a water bath before samples were subjected to a two-stage homogenization (20/5 MPa) using a high-pressure homogenizer (Panda plus 1000, GEA Niro, Soavi, Italy).

Subsequently, each of the samples were divided in aliquots of 20 mL in 50 mL centrifuge tubes and subjected to a heat treatment at 90 °C for 10 min in a water bath. The selected condition of heat treatment followed our previous study and emulates what is applied in industrial yogurt production (85–90 °C for 5–10 min) (Walstra, Walstra, Wouters, & Geurts, 2005; Li et al., 2021b). During this step, samples were collected after 0, 2, 5, and 10 min for SAXS measurements as described below. Samples were cooled down to ~ 10 °C in an ice water bath before analysis.

After the heat treatment (90 °C for 10 min), acidification was induced by addition of 1.5% (w/v) GDL (glucono- δ-lactone; Sigma Aldrich Co., St Louis, MO, USA). The samples were initially shaken gently for 30 s and then kept in a water bath at 45 °C until the pH reached 4.60 ± 0.05. This was monitored using a HQ411D Laboratory pH mV^{-1} Meter with an Intellical™ PHC705 electrode (Hach, Düsseldorf, Germany) and pH was measured in triplicate. The relation between

Table 1
Experimental design and ingredients used in the non-fat acidified milk model systems.

Total protein content (%, w/w)	No.	Model system code	Total casein (LCC) (%, w/w)	Total whey protein (%, w/w)	LWPC (%, w/w)	NWP (%, w/w)	WPC (%, w/w)
4	1	LCC	4.0	–	–	–	–
	2	LWPC	–	4.0	4.0	–	–
	3	LCLW	2.0	2.0	2.0	–	–
	4	W^1	2.0	2.0	0.5	–	1.5
	5	W^2	2.0	2.0	1.0	–	1.0
	6	N^1	2.0	2.0	0.5	1.5	–
	7	N^2	2.0	2.0	1.0	1.0	–
3.5	8	SM	2.8	0.7	0.7	–	–
	9	Com SM	Skim milk, commercial				

Note: LCC represent liquid casein concentrate, LWPC represents liquid whey protein concentrate, NWP is nano-particulated whey protein, and WPC is whey protein concentrate. The calculated protein composition ignores the small amount of whey protein and casein content existing in LCC and LWPC, respectively.

pH and time was found to be logarithmic (seen in equation (1)) during acid gelation with R^2 values ranging from 0.995 to 0.999.

$$pH = A^{*}ln(t) + B \quad (1)$$

where t represents time in min. The values of A and B varied slightly for the different model systems (data not shown).

2.3. Small-angle X-ray scattering (SAXS)

The measurements during heat treatment were performed using a GANESHA instrument from SAXSLAB (Lyngby, Denmark) with a Rigaku (Rigaku-Denki, Co., Tokyo, Japan) 40 W micro-focused Cu source producing X-rays. A wavelength of λ = 1.54 Å was detected by a moveable Pilatus 300 k pixel-detector from Dectris (Baden, Switzerland), which is capable of measuring different angular ranges and thus length scales. The two-dimensional scattering data were azimuthally averaged using standard reduction software (SAXSGUI, Lyngby, Denmark). The scattering patterns for the radially averaged intensity (Int.) from the detector were recorded as a curve against the scattering vector q = 4π*sinθ/λ, where λ is the x-ray wavelength, and 2θ is the scattering angle. q was recorded in the range of 0.005–0.3 $Å^{-1}$. Each of the samples collected after 0, 2, 5, and 10 min of heat treatment was transferred to a borosilicate capillary tube with a syringe and measured at 25 °C with an acquisition time of 1 h. The data shown in this study are the corrected spectra after subtraction of the buffer background (permeate).

The structural changes during acidification were measured using a Nano-inXider from Xenocs SAS (Grenoble, France) which also uses a Cu K_α source and a two-detector setup for simultaneous SAXS /Wide angle X-ray scattering (WAXS) measurements also with a 1.54 Å wavelength. After the heat treatment (90 °C, 10 min), each sample was mixed with GDL 1.5% (w/v) and loaded into borosilicate capillary tubes. Following 5 min of evacuation in a desiccator at room temperature, the samples were measured at 45 °C with a total acquisition time of around 100 min (18 cycles of 5 min interval each). The setting of very high resolution (VHR) was chosen with a beam size of 200 μm. The q range was recorded from 0.004 to 0.3 $Å^{-1}$. The equipped XSACT software was applied for background subtraction (permeate in this study), and data were logarithmically re-binned.

All the SAXS data are presented in log I(q) - log q plots. The selected three q ranges, low-q (0.004–0.005 $Å^{-1}$), Intermediate-q (0.009–0.04 $Å^{-1}$), and high-q (0.08–0.1 $Å^{-1}$) were applied based on the SAXS scattering data from this study.

Variation of scattering intensity I(q) within the same sample can be inferred based on the following general equation.

$$I(q) = \Delta\rho^2 n_p V_p^2 P_P(q) S(q) \quad (2)$$

where $\Delta\rho^2$, n_p, V_p and $P_p(q)$ are the contrast, number density, volume and form factor of the particle in question, respectively; q is the length of the scattering vector, and S(q) is the structure factor describing any interactions between particles. S(q) equals 1 in a dilute system, which we will assume here.

The SAXS scattering data of a whey protein-only system LWPC was analyzed using the SasView package, v. 5.0.4 (http://www.sasview.org/), which aims to give insight or indication on the shape or surface of the scattering object. Two fitting models were used, a model of ellipsoids was applied during the higher q range from 0.07 to 0.2 $Å^{-1}$ and a unified model (unified_power_Rg) was used to fit the lower q range from 0.005 to 0.07 $Å^{-1}$.

The ellipsoid model has been developed by (Fejgin & Svergun, 1987), and the equations are as follows:

$$P(q,\alpha) = \frac{scale}{V} F^2(q,\alpha) + background \quad (3)$$

where.

$$F(q,\alpha) = \Delta\rho V \frac{3(sin(qr) - qrcos(qr)}{(qr)^3} \quad (4)$$

and.

$$r = [R_e^2 sin^2\alpha + R_p^2 cos^2\alpha]^{1/2} \quad (5)$$

α is the angle between the axis of the ellipsoid and q, and $V = (4/3)\pi R_p R_e^2$ is the volume of the ellipsoid. Here R_p is the polar radius, and R_e is the equatorial radius. Δρ (contrast) is the scattering length density difference between the scatterer and the solvent.

The unified_power_Rg model adopts the empirical multiple level unified Exponential/Power-law fit method, which is developed by Beaucage (1996). Here the intensity is given by.

$$I(q) = background + \sum_{i=1}^{N} [G_i exp\left(-\frac{q^2 R_{gi}^2}{3}\right) + B_i exp(-\frac{q^2 R_{g(i+1)}^2}{3})(\frac{1}{q_i^*})^{P_i}] \quad (6)$$

where.

$$q_i^* = q[erf\left(\frac{qR_{gi}}{\sqrt{6}}\right)]^{-3} \quad (7)$$

R_{gi} is the radius of gyration, G is the Guinier prefactor, B is a prefactor specific to the type of power-law scattering, and P = -4 in Porod's law used in this study. For each level, the four parameters G_i, R_{gi}, B_i and P_i were chosen.

The selected scattering data from heat treatment were fitted to a polydisperse sphere model in the q range from 0.008 to 0.05 $Å^{-1}$. The following equation was applied for calculation (Yang et al., 2021).

$$P_{PS}(q) = \int P_S(q) D(R) V(R)^2 dR \quad (8)$$

where the monodisperse sphere form factor is given by.

$$P_S(q) = [3\frac{sin(qR) - qRcos(qR)}{(qR)^3}]^2 \quad (9)$$

The log-normal distribution follows.

$$D(R) = \frac{1}{R\sigma\sqrt{2\pi}} exp(\frac{-[ln(\frac{R}{R_0})]^2}{2\sigma^2}) \quad (10)$$

where σ is the variance and R_0 is the geometric mean of the log-normal distribution; V(R) is the sphere volume and R is radius of the spheres.

2.4. Statistical analysis

SPSS Statistics 27 (IBM, New York, USA) was used for statistical analysis in this study. ANOVA (one-way analysis of variance) was done following Tukey's multiple comparison test based on a statistical significance level of $P < 0.05$.

3. Results and discussion

3.1. Heat treatment

Fig. 1 presents an overview of background subtracted SAXS data from the different milk model systems listed in Table 1. These were all subjected to heat treatment (90 °C) for 0, 2, 5, and 10 min. From Table 1 we see that the casein-only system (LCC) and the pure whey protein sample (LWPC) can be considered the building blocks of the remaining samples so we will describe their behavior first and then turn to the mixed samples.

3.1.1. LCC and LWPC samples

The casein-only system (LCC) only exhibited slight changes in the

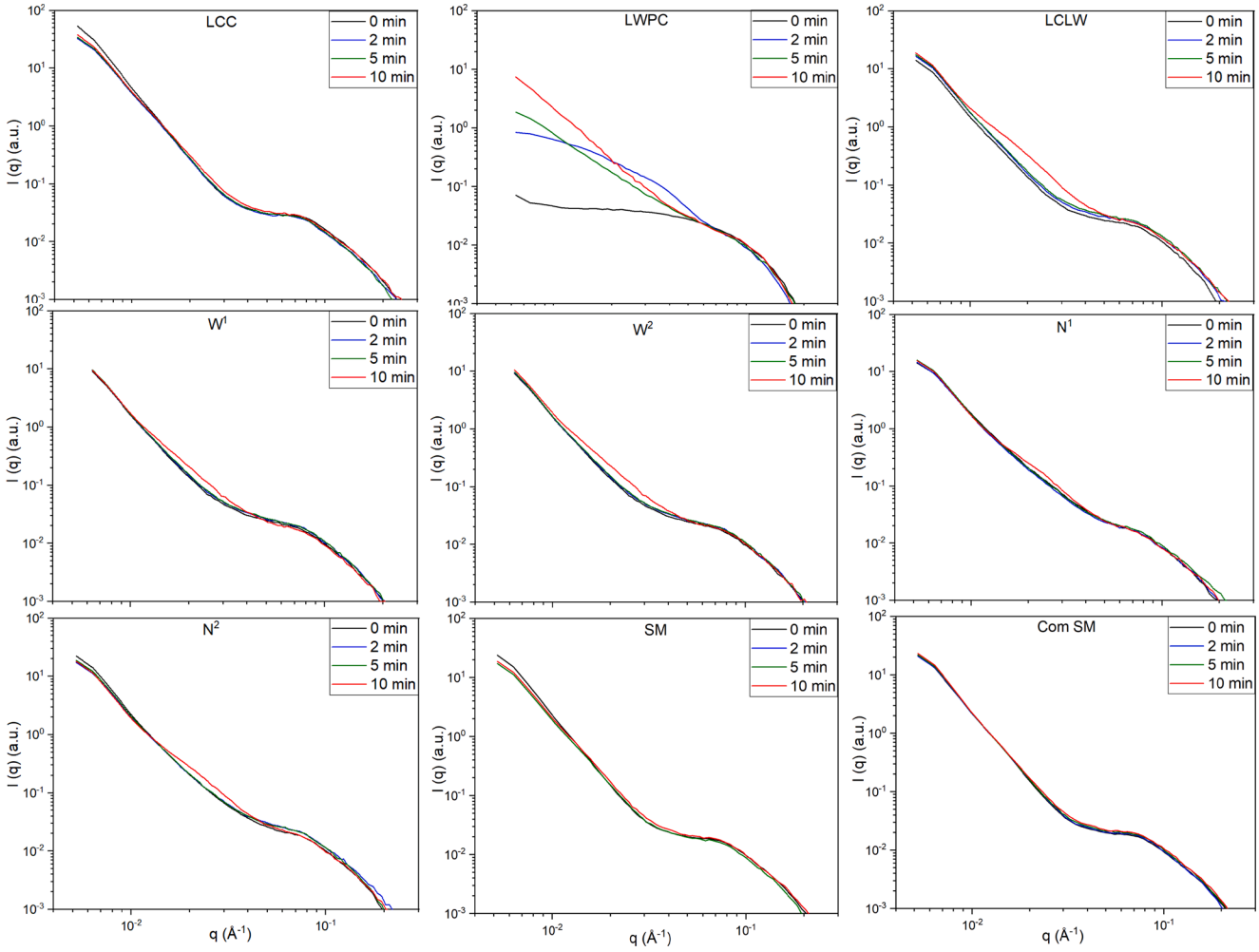

Fig. 1. Background-subtracted SAXS data of different milk model systems after heat treatment (90 °C) 0, 2, 5, and 10 min, as indicated in the legend. The descriptions of the systems are given in Table 1.

scattering data, which is not surprising since the overall internal structure of casein micelles is not expected to be markedly disrupted at temperatures below 120 °C at the native pH of milk (pH 6.7) (Dalgleish & Corredig, 2012). However, the system containing only whey protein (LWPC), showed significant changes in the scattering data with increasing heat treatment time, particularly at low q. We attribute this to some level of denaturation or surface disruption and subsequent aggregation of whey protein at the applied temperature of 90 °C. A model combining a local ellipsoidal shape to describe the individual protein contour and the unified model to describe larger aggregates were applied to interpret the scattering of LWPC (Fig. 2). The ellipsoid can be taken to represent the local shape of whey proteins in LWPC with dimensions matching those of the known crystal structure of β-lactoglobulin (PDB ID 1BEB), which is the major whey protein. The scattering data show that this local structure is basically preserved during the heat treatment as evident from the unchanged scattering at q-values larger than ca. 0.07 $Å^{-1}$ during the entire heat treatment duration of 10 min (note the unchanged radius of the ellipsoid shape in Table 2). A partial denaturation where the overall shape is largely preserved, but where protein parts exposed on the surface are mainly affected and could induce aggregation, would explain the obtained scattering data.

The aggregation is evident from the behavior at q-values lower than ca. 0.07 $Å^{-1}$ where significant changes occur over the course of the heat treatment. At 0 min there is a slight upturn in the intensity at the lowest q-values, indicating the presence of a small amount of larger aggregates (Fig. 2), but overall the scattering here is fully described by the local

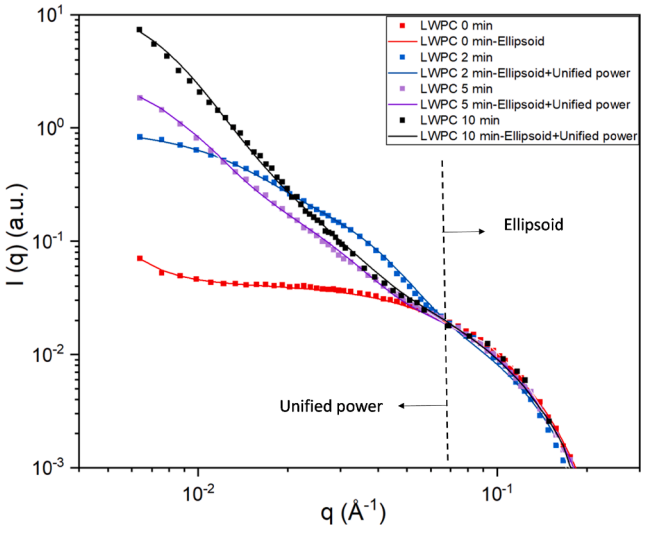

Fig. 2. Background-subtracted SAXS data of LWPC with data fitting after heat treatment (90 °C) 0, 2, 5, and 10 min, as indicated in the legend. LWPC represents liquid whey protein concentrate producing from ultra-filtration.

Table 2
Fitting parameters of a model combining an ellipsoidal shape and the unified model for the scattering of LWPC.

Time/ min	Ellipsoid					Unified power						
							B-level 1			B-level 2		
	A-scale	A-radius-polar (nm)	A-radius-equatorial (nm)	B-scale	B-Rg1 (nm)	B-power1	B-B1 (cm^{-1})	B-G1 (cm^{-1})	B-Rg2 (nm)	B-power2	B-B2 (cm^{-1})	B-G2 (cm^{-1})
0	0.0064	5	1.7	–	–	–	–	–	–	–	–	–
2	0.0064	5	1.7	0.001	5.5	4	4.50E-08	260	14	4	4.50E-09	700
5	0.0070	5	1.7	1	7	4	4.50E-08	0.15	45	4	7.75E-09	1
10	0.0070	5	1.7	1	10	4	4.50E-08	0.6	60	4	1.47E-08	50

Note: Scale: means scale factor or volume fraction; Rg is radius of gyration.

ellipsoidal shape. As the heat treatment progresses, the unified model fits indicate the presence of two size populations evolving as described by the fitted radii of gyration (Rg). These numbers go from 5.5 nm / 14 nm (2 min) to 7 nm / 45 nm (5 min) and finally 10 nm / 60 nm after 10 min (Table 2). The increasing sizes of aggregates observed here show that most of the native whey protein is affected by the heat treatment in a way that favors aggregation into larger structures, but whether the proteins are fully denatured is not clarified - if so, the overall nanoscale shape remains relatively unchanged as mentioned above. Corresponding to the fitting parameters of LWPC in Table 2, a schematic model of LWPC structural changes can be seen in Fig. 3, where it is illustrated how native whey protein gradually change during heat treatment.

The denaturation ratio of total native whey protein in skim milk samples has previously been found to be around 85–90% at 90 °C/10 min at pH 6.55 using a thermostatically controlled oil bath (Anema & Li, 2003). Qian et al. (2017) also found the denaturation degree of whey proteins in raw milk to be around 80% at 85 °C and 100% at 95 °C after 10 min using a water bath and Native-PAGE measurements. It is however unclear from these studies how the structure of the proteins were affected during the applied treatments. Assuming a similar level of denaturation in our system, we can conclude from the above that the heat treatment mainly affects the surface of the whey proteins, but does not lead to a complete unfolding within the time frame observed here.

3.1.2. *Mixed systems, LCLW, $W^{1/2}$ and $N^{1/2}$*

For all the mixed milk model systems, with a total casein content of 2 % and a total whey protein content of 2% (i. e., LCLW, W^1, W^2, N^1 and N^2), we primarily find significant changes in the intermediate-q range (0.009–0.04 $Å^{-1}$) during heat treatment (Fig. 1). Given the results from the pure casein and whey protein systems described above, we conclude that these changes are mainly due to whey protein alterations. We can extract more detailed information by treating the time 0 min of each model system as a background, and subtracting them from the scattering curve obtained at time 10 min. The resulting curves in the intermediate-q range of 0.009–0.04 $Å^{-1}$ were subsequently modelled as polydisperse spheres as shown in Fig. 4 A. Fig. 4 B and C present the particle size distributions and average radius, respectively, for the different model systems. All the particle sizes, after heating 10 min, ranged from ca. 2 to 20 nm in radius in the intermediate-q, apart from the pure LCC, which basically remained unchanged as mentioned above.

Two questions seem relevant: do the different whey protein components behave similarly, and to what extent do they interact with caseins? Fig. 4 B reveals the following progression of particle size formation between the mixed samples: SM/Com SM < $W^{1/2}$ < LCLW < $N^{1/2}$.

Apart from the self-interactions demonstrated above in the LWPC sample, whey proteins can aggregate together with micellar or serum κ-casein and α_{s2}-casein, with sizes of formed complexes ranging from 30 to 100 nm (diameter) during heat treatment (Donato & Dalgleish, 2006; Donato, Guyomarc'h, Amiot, & Dalgleish, 2007), while deviation may occur due to the different measurements of particle sizes applied compared to the present study. It has also been reported that only around 30 % of the denatured whey proteins attach to casein micelles and the rest exist as soluble complexes in the solution at the natural pH of milk (Kethireddipalli, Hill, & Dalgleish, 2010). Thus, it may be speculated that most of the particle sizes (radius around 3–20 nm) found in the present study are likely to represent soluble denatured whey protein-whey protein aggregates although the association of whey protein and individual caseins may also occur. In particular, compared to the pure LWPC sample, the mixed system LCLW (2% LCC and 2% LWPC) presented a larger average radius of ~8 nm (versus ~ 6 nm). It can thus also be proposed that the formed whey protein aggregates (LWPC) were affected by the presence of casein (LCC), e.g., forming complexes with individual caseins during heating. Both W^1 and W^2 presented a similar particle size distribution as seen for LCLW, but with lower average radius than LCLW. This may suggest a similar aggregation behavior of WPC as for LWPC, but with more native whey protein in LWPC leading to more exposed bonds available for interaction with other proteins during heating. Furthermore, it was reported by the manufacturer that the WPC powder also contained ~ 17% caseinomacropeptide (CMP) as it was produced from whey stemming from cheese production. CMP will not denature/aggregate during heat treatment. Both N^1 (0.5% LWPC

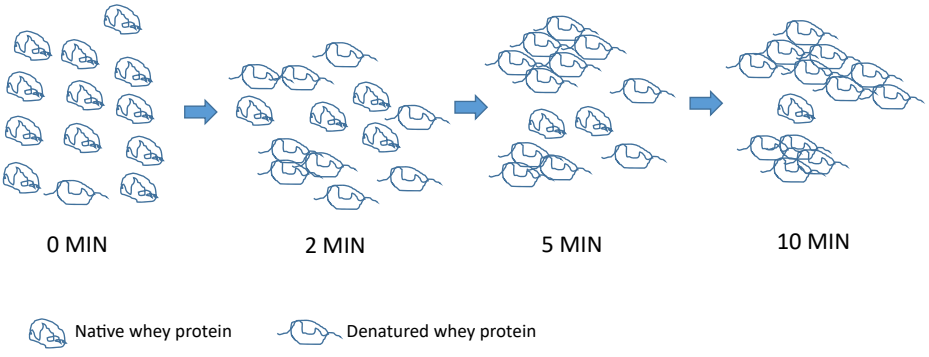

Fig. 3. Schematic of LWPC structural development with increasing heat treatment (90 °C) time from 0 to 10 min. LWPC represents liquid whey protein concentrate produced from ultra-filtration.

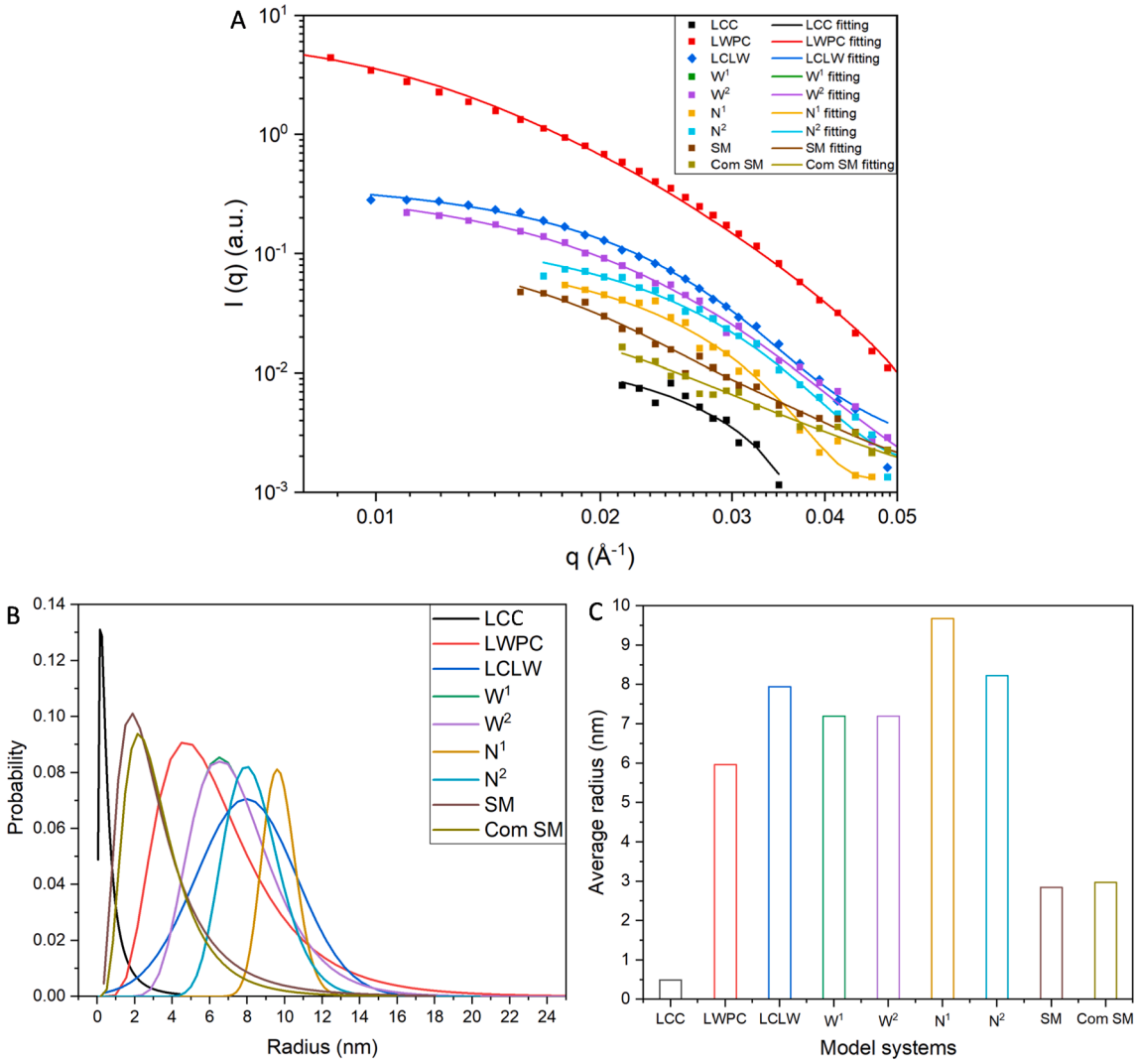

Fig. 4. Major differences among the different milk model systems during heating, represented by selected scattering curve with data fitting from 0.008 to 0.05 Å^{-1} (A), and their corresponding particle size distributions (B) and average radius (C).

and 1.5% NWP) and N^2 (1% LWPC and 1% NWP) demonstrated relatively narrow particle size distributions and increased particle sizes after heating compared to LCLW, W^1 and W^2. N^1 exhibited the highest average radius with narrower distribution, which may imply that heating induced larger NWP-NWP, or NWP-LWPC, aggregates formed in N^1. N^2 presented lower average radius of ~ 8 nm compared to ~ 9.5 nm for N^1 during heating. NWP has previously been shown to exhibit larger aggregate sizes compared to systems with added either micro-particulated whey protein (MWP) or WPC. It has been suggested that NWP has a large surface area because of its original small size (Li et al., 2021b).

A simplified quantitative view of the effect of the heating time can be obtained by looking at the intensity development at a single selected q-value of ~ 0.025 Å^{-1} as shown in Fig. 5. The intensity values were normalized to the initial intensity value at time 0. The most significant effect after 10 min is seen for the LCLW sample, but interestingly only the W$^{1/2}$ samples exhibit any sign of aggregation after 2 and 5 min of heating. As mentioned above, these samples show similarities in the size distributions after 10 min of heating, but the time evolution suggests that the W$^{1/2}$ samples are slightly more susceptible to heat induced surface modifications. Apart from the W$^{1/2}$ samples, all samples have to be heated for more than 5 min to show any detectable aggregation behavior.

3.1.3. *Skim milk references SM and Com SM*

The skim milk samples (SM and Com SM) did not show significant differences during heating. Two reasons for this seems likely: first, these samples contain only 0–0.7% whey proteins compared to 2% in the other samples, reducing the probability for whey proteins to associate in solution. Second, as seen in equation (2) above, the scattering intensity scales both with the square of the particle volume and the particle concentration, thus the casein micelles dominate the spectrum until whey protein aggregates reaches a certain level depending on size and number of particles.

3.2. *Acidification*

An overview of the SAXS scattering data obtained during acidification for each of the model systems can be seen in Fig. 6. Further, in Fig. 7 A and B, the intensity evolution as a function of pH is shown for two selected q-values. A quick glance of Fig. 7 B shows that the samples again fall into groups with similar behavior, namely the high casein containing samples LCC/SM/Com SM, the W$^{1/2}$ and LCLW samples, the N$^{1/2}$ samples and finally the pure whey sample LWPC.

3.2.1. *LWPC sample*

The most striking changes are the gradual smoothing of high-q features and an overall intensity reduction with decreasing pH for all the

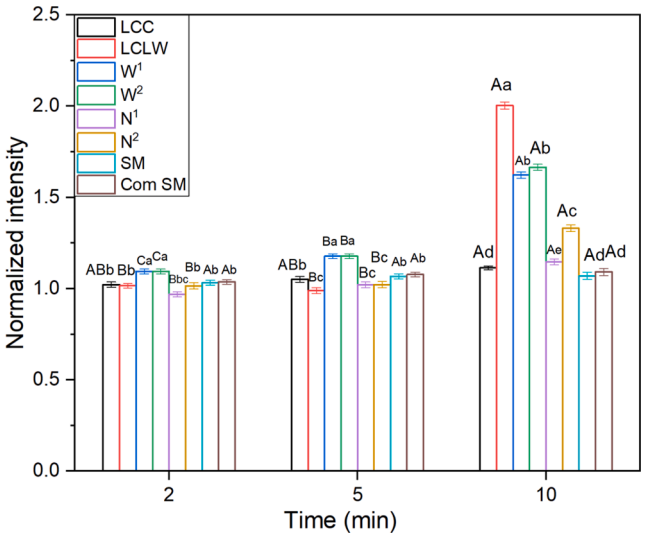

Fig. 5. Changes of scattering intensity after heating 2, 5 and 10 min compared to the original sample (0 min) at q = 0.025 Å^{-1}. Values were calculated by dividing the intensity of original sample (0 min heat treatment). Each error bar is the mean ± SD (n = 2); values with uppercase letters represent significant difference between heating time, and lowercase letters mean significant difference between different model systems at the same heating time (P < 0.05).

model systems, except for the whey protein-only sample, LWPC, which almost maintains its initial local structure during the entire acidification process. Thus, opposite to what was observed for the heat treatment, the whey proteins are largely unaffected by the acidification as quantified by basically constant intensity values in Fig. 7 A and B.

3.2.2. LCC and SM/Com SM samples

For the LCC sample and the other two high casein containing samples SM/Com SM the situation is opposite as the scattering curves change both in intensity and shape. Changes in high-q (0.08–0.1 Å^{-1}) features represent primarily local protein inhomogeneities (De Kruif, 2014; Ingham et al., 2016) and were most pronounced in the casein-only sample LCC (4% casein), and the two references SM and Com SM (2.8% casein) compared to the other mixed systems (2% casein). Fig. 7 shows that the intensity development is different at high and low q. At high q the intensity drops roughly linearly with pH while at low q the intensity drops steeply around a pH of ca. 5.2. Again, with reference to equation (2), there can be several reasons for changes in the intensity: the size and number of objects, but also the contrast (Δρ) given by the difference in electron density of the proteins and the surrounding medium. In this case, contrast changes can be caused by the release of calcium from the casein micelles into the serum phase as well as a general disruption of the micelles, creating a more uniform protein solution. However, there are also clear structural changes occurring: at the lowest q-values the shape of the curve initially contains a distinct signature of the overall casein micelle size from the curvature of the

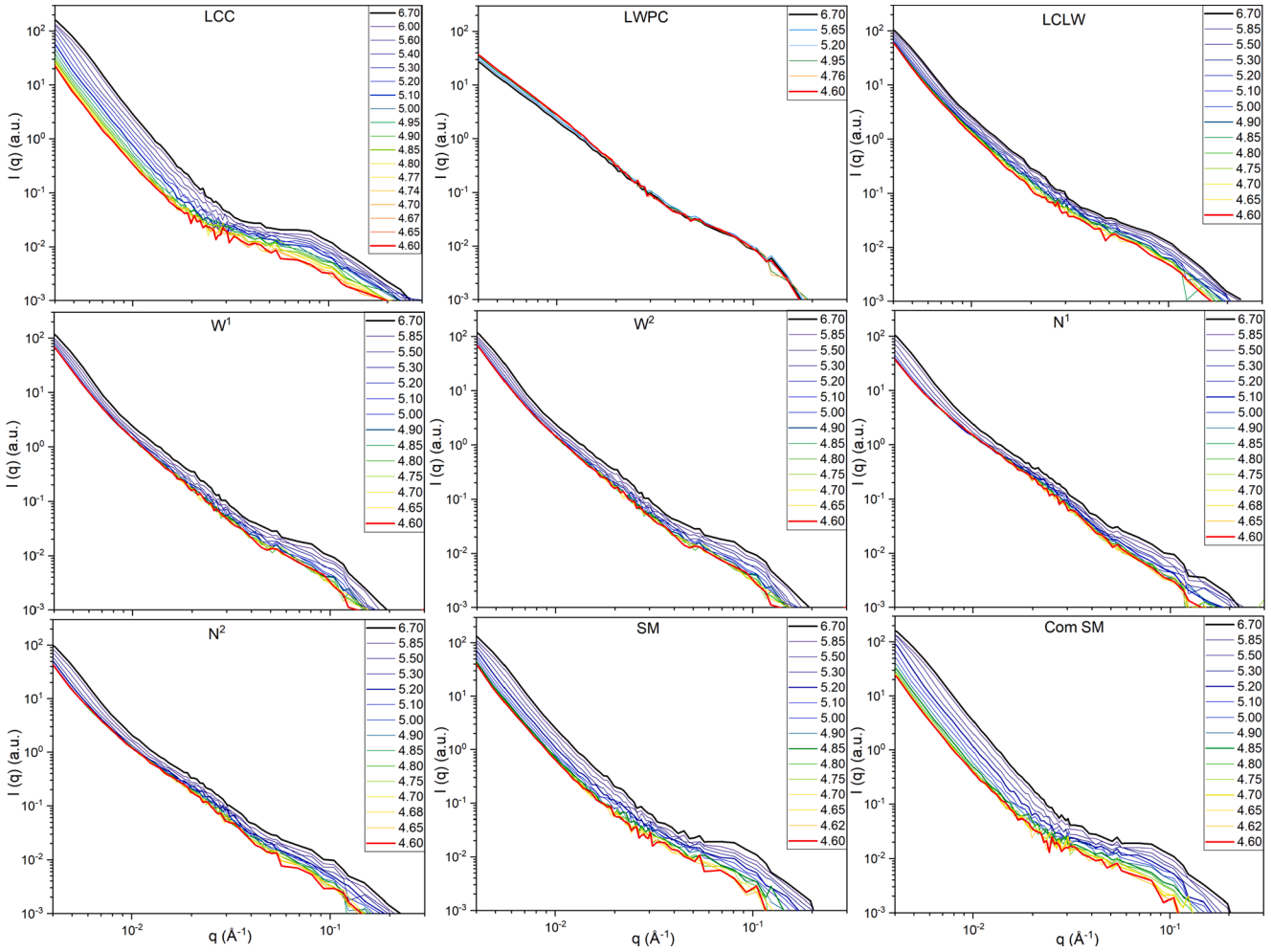

Fig. 6. Background-subtracted SAXS data of different milk model systems at different pH, as indicated in the legend, during acidification. The descriptions of the systems are given in Table 1.

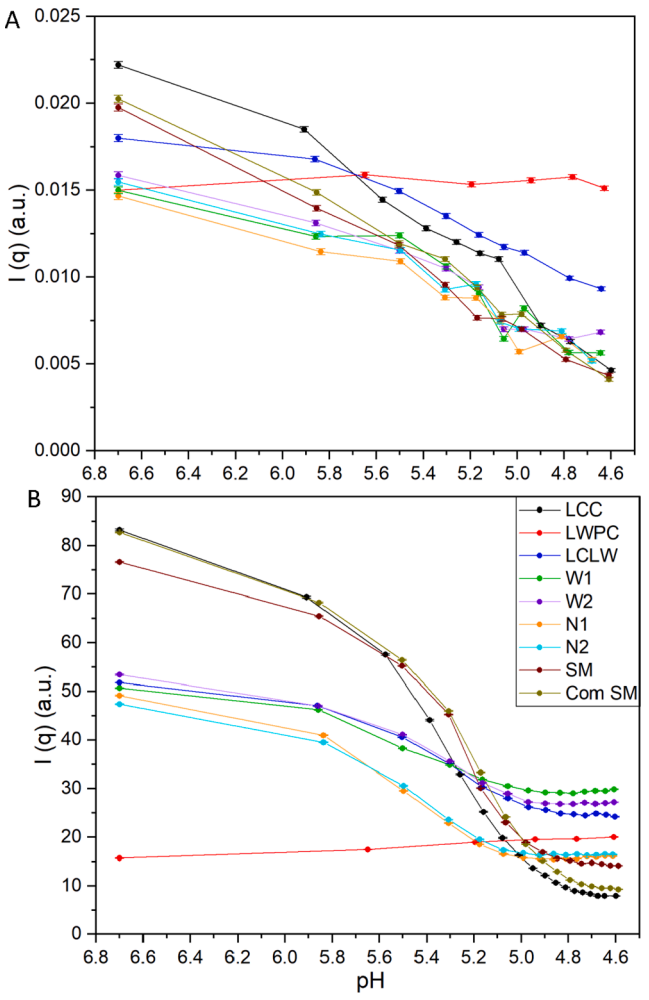

Fig. 7. Changes of scattering intensity of different milk model systems at different pH during acidification at the selected q value of 0.08 $Å^{-1}$ (A) and 0.005 $Å^{-1}$ (B).

data. This curvature is gradually lost indicating most likely a micellar breakdown or at least a loosening, potentially leading to larger structures outside the resolution of our instrument. Also, increasing aggregate size could also lower the intensity as large aggregates would sediment out of the x-ray beam (Ingham et al., 2016).

In fact, pH values of 5.2–5.1 corresponds to a region where the structure of casein micelle loosens, CCP is completely solubilized into the serum phase and phosphoproteins are redistributed. Ingham et al. (2016) also mentioned a similar phenomenon of broader high-q features appearing in skim milk at pH 5.15 during acid gelation using GDL. During milk acidification, a specific demineralization, i.e., a progressive release of CCP from the interior of the casein micelles and dissolving into the serum phase at pH dropping from 6.7 to 5.3 has been observed by Marchin et al. (2007). Casein micelles have been reported to become smaller, more homogeneous and have a higher average density from pH 6.5 to 5.2 during skim milk acidification (Moitzi, Menzel, Schurtenberger, & Stradner, 2011) with a subsequent disappearance of the high-q feature at pH 4.85. The explanation put forward was, that already released casein in the serum aggregated at the low pH, providing a more uniform structure in this high-q region (Ingham et al., 2016; Moitzi et al., 2011). These observations generally make sense also for our data.

3.2.3. *Mixed systems, LCLW, $W^{1/2}$ and $N^{1/2}$*

In comparison to LCC and the references (SM and Com SM), the mixed systems containing 2% of casein and 2 % of whey protein (i. e., LCLW, W^1, W^2, N^1 and N^2) showed less evident high-q feature decreasing rate (Fig. 7A). The low-q behavior however, also shows a decrease similar to the LCC sample, but with reduced rate and for the $N^{1/2}$ samples at a slightly higher pH, ca. 5.4.

In addition, the overall intensity reduction rates of mixed systems (i. e., LCLW, W^1, W^2, N^1 and N^2) seems less significant compared to LCC and the references (SM and Com SM). This may be related to both the different varying rate of reduced contrast and casein micelle structure disruption, and relatively smaller casein-whey protein aggregates forming during acidification compared to larger casein-casein aggregates in LCC and the skim milk references.

From the overview of SAXS scattering in the low-q range (0.004–0.005 $Å^{-1}$), all the model systems, except LWPC, showed a small deviation at the natural pH (6.7), which was related to a comparatively rough surface of casein micelles based on the study by Liu et al. (2017)a. They found that the small positive deviation followed Porod's law at natural pH of skim milk. The interfacial scattering intensity after this deviation, i.e. the low- q range decayed by a q^{-4} power law during acidification with GDL, where a relatively smooth and sharp interface was gradually formed as pH was decreasing. Besides, they confirmed these structural characteristics of casein micelles before and after acidification using transmission electron microscopy (TEM) and explained the changes as a result of concomitant gradual shrinkage of κ-casein hairy layers. Thus, the interface of the casein micellar structure in the studied model systems may also become more smooth and sharp with decreasing pH in the present study. The scattering intensities of LCC, and the two references (SM and Com SM) were lower than for the other mixed systems (LCLW, W^1, W^2, N^1 and N^2) below pH 5.0 at a selected low-q around 0.005 $Å^{-1}$, seen in Fig. 7B. This might imply that larger casein-casein aggregates formed after demineralization. In addition, compared to LWPC, the intensities of LCLW were much higher even though they kept decreasing with decreasing pH. It cannot be directly confirmed that LWPC interacted with LCC, forming casein-whey protein aggregates larger than the whey protein-whey protein aggregates present, but smaller than casein-casein aggregates (present in LCC). The general decreasing intensities and rate of LCLW were similar to W^1 and W^2, except at lower pH values from 4.8 to 4.6, where its intensity was slightly lower. This could indicate slightly larger casein-WPC aggregates forming in this range. The intensities of systems with added NWP (N^1 and N^2) decreased more significantly than LCLW, W^1 and W^2 from pH 6.7 to 4.6 (Fig. 7B). NWP has been reported to self-associate at pH ≥ 5.5 caused by decreased electrostatic repulsion and enhanced hydrophobic interaction (Liu et al., 2017b).

The mixed systems (LCLW, W^1, W^2, N^1 and N^2) showed a second (less distinct) inflection point at around 0.009 $Å^{-1}$, which was not seen for LCC and the two references (SM and Com SM) (Fig. 6). The inflection points disappeared at around pH 5.2, when dense proteins disrupt (casein micelles loosen). This may indicate that more added whey protein may induce changes to the structure of casein clusters by interacting with caseins as seen from the intermediate-q range (0.009–0.04 $Å^{-1}$) from pH 6.7 to 5.2.

3.3. *General discussion*

Schematic diagrams of interactions between the proteins in the selected three different model systems (i.e., LCLW, W^1, N^1) during both heating and acidification are shown in Fig. 8. The diagrams are based on both the discussion of obtained SAXS scattering data in the present study and on previous studies (Ingham et al., 2016, Li et al., 2021b, Liu et al., 2016), suggesting a possible interaction mechanism of the selected proteins from changes of their local protein structure. The casein micelle model chosen is the one suggested by Ingham et al. (2016) considering a hydrated sponge-like structure. K-casein on the surface ensures that the micelle is stable against aggregation, and the chains of casein-omacropeptide (CMP) are extended from the micellar surface and anchored as a hairy layer, providing steric stabilization of the micelles.

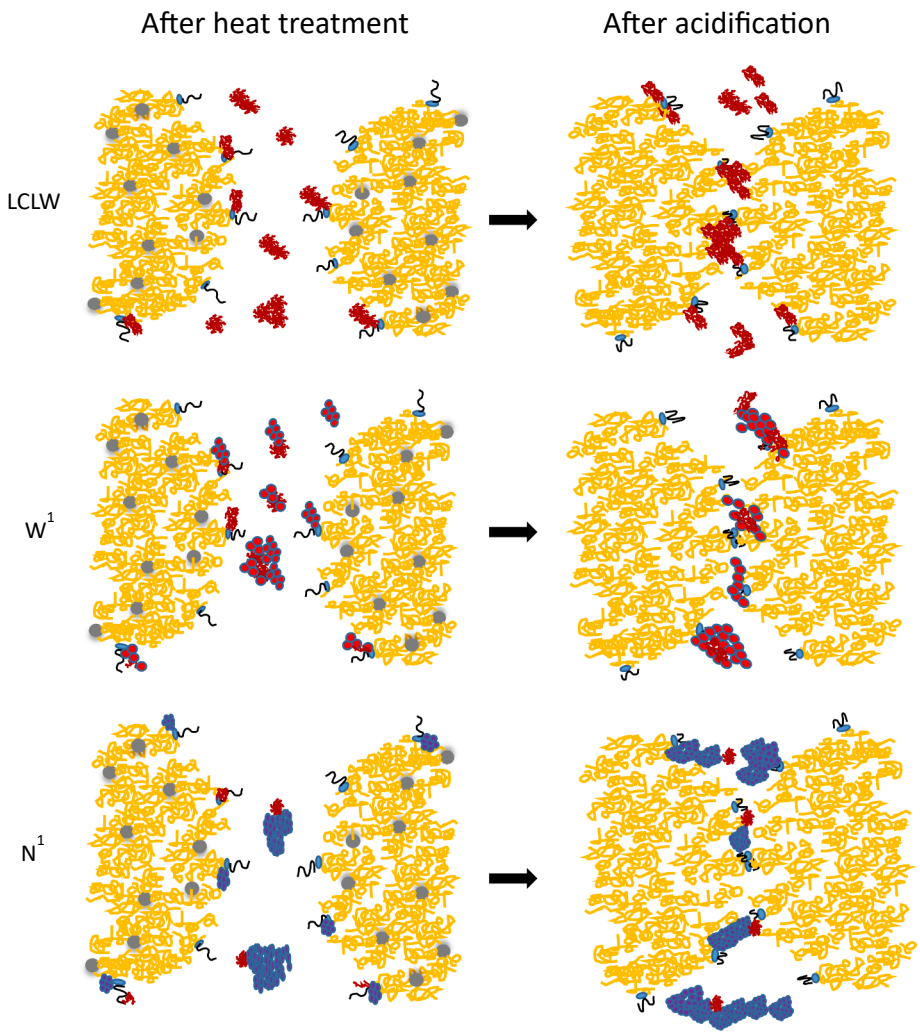

Fig. 8. Diagrams of interacting caseins with different types of whey proteins during processing of acidified gels (only the interacting parts are shown, not the whole particles). α_s- and β-caseins are represented by yellow hairs. κ-casein is blue, the caseinomacropeptide chains are black, and calcium phosphate nanoclusters are represented by grey spheres. Inherent whey protein (LWPC) are in red hairs, NWP are purple spheres, and WPC are red spheres. Not drawn to scale.

After heat treatment, some of the whey proteins are able to form disulphide bonds with κ-casein in the inner part of the casein micelle by penetrating the layer of CMP (Donato et al., 2007), and others aggregate themselves or with individual caseins in the serum, which are illustrated in Fig. 8. Meanwhile, the complexes of whey protein-κ-casein in the inner part of the casein micelle are reported to be also capable of preventing coagulation of casein micelles, resulting in their stability in milk solution (Dalgleish & Corredig, 2012). In addition, the complexes can facilitate additional attachment points between micelles during acid gelation (Ingham et al., 2016). Based on the discussion of SAXS changes for the different systems above, heat treatment did not markedly affect the overall structure of casein micelles (e.g. LCC). However, it caused significant changes to all mixed systems (LCLW, W^1, W^2, N^1, and N^2) with whey protein included, mainly in the intermediate-q range of 0.009–0.04 $Å^{-1}$ with particles sizes ranging from 1 to 20 nm (radius). Most soluble denatured whey protein aggregates can be assumed to form in the serum phase, which were observed in this intermediate-q range. More LWPC-LWPC aggregates were formed after heat treatment of 10 min, as the structure of native whey proteins changes to a greater degree when getting denatured and aggregating. The behavior of WPC was similar to LWPC, because WPC also contains a small amount of native whey protein, leading to formation of more disulphide bonds after heating than NWP. NWP mostly includes denatured whey protein aggregates produced in nano size and the small particles may already aggregate in the solution before heating because of higher surface area. Subsequently, the NWP aggregates continue to attach to other proteins, forming larger aggregates during heating. The higher average radius with narrower distribution in the system with added NWP may imply that larger NWP-NWP, NWP-LWPC, or even LWPC-LWPC aggregates were formed during heating. It has also previously been reported that the average particle size of a model system with added WPC was only slightly higher than that with added LWPC, but significantly lower than that with NWP, when they were mixed with the same amount of casein (Li et al., 2021b). NWP was also suggested to interact with other proteins, like casein and whey protein isolates (Liu et al., 2016).

During acid gelation, the steric stabilization of micelles will decrease with the decreasing pH, where the κ-casein layer collapses due to the decreasing charge of CMP (De Kruif, 1999). This can be inferred from the small deviation at low-q features (0.004–0.005 $Å^{-1}$), and high-q features disappearing at pH ~ 5 for almost all model systems with added LCC in this study. The micelles can then connect at a closer range because of the attractive forces (Dalgleish & Corredig, 2012). As indicated in Fig. 8, the overall structure of micelle aggregates in the three model systems became more compact and denser during acidification. The decreasing overall intensity of SAXS scattering may also imply an increase in larger aggregates formed during acidification, which are sedimented out of solution and not detected by the X-ray beam for the model systems of LCLW, W^1, and N^1. The intensity of SAXS scattering decreased more

significantly for N^1 compared to LCLW and W^1 at low q-range, meaning that NWP may form larger aggregates during acidification, as indicated in Fig. 8.

4. Conclusion

Structural changes of milk model systems with added whey protein ingredients induced by heat treatment and acid gelation were investigated using SAXS. Overall, heat treatment was found to mainly affect whey protein components, and acidification mainly affected caseins. In mixed systems of both casein and whey proteins, the structure formation and dynamics can be influenced by the form of the added whey protein components. The formation of a larger structure was obtained for systems containing NWP compared to WPC during heat treatment. The NWP containing samples also showed structural changes at slightly higher pH values than the WPC samples during acidification. The pure liquid whey protein (LWPC) samples was affected significantly through denaturation and resulting aggregation by heat treatment, the modeling of its SAXS data presented mainly a surface effect leaving the overall protein shape and dimensions unaffected. A mechanism for the protein interactions was suggested based on their different internal structural changes during both heat treatment and acidification, and combined with previous findings. SAXS was shown to be a promising non-destructive method to probe turbid samples, like the acidified gels in the present study, evaluating their original structures without disruption, which would not be possible with conventional light scattering techniques.

CRediT authorship contribution statement

Ruifen Li: Conceptualization, Methodology, Formal analysis, Investigation, Validation, Writing – original draft. **Tanja Christine Jæger:** Conceptualization, Writing – review & editing, Funding acquisition. **Tijs A.M. Rovers:** Conceptualization, Resources, Writing – review & editing, Funding acquisition. **Birte Svensson:** Conceptualization, Writing – review & editing, Funding acquisition. **Richard Ipsen:** Conceptualization, Methodology, Validation, Writing – review & editing, Supervision, Project administration, Funding acquisition. **Jacob J.K. Kirkensgaard:** Conceptualization, Methodology, Validation, Writing – review & editing. **Anni Bygvrå Hougaard:** Conceptualization, Resources, Validation, Writing – review & editing, Supervision, Project administration, Funding acquisition.

Declaration of Competing Interest

The authors declare that they have no known competing financial interests or personal relationships that could have appeared to influence the work reported in this paper.

Acknowledgements

This research was jointly supported by the Danish Dairy Research Foundation and Chinese Scholarship Council, CSC. Arla Foods Ingredient (Nr. Vium, Denmark) is thanked for providing nano-particulated whey protein and whey protein concentrate powders. SAXS data was generated via a research infrastructure at University of Copenhagen, partly funded by FOODHAY (Food and Health Open Innovation Laboratory, Danish Roadmap for Research Infrastructure).

References

Anema, S. G., & Klostermeyer, H. (1997). Heat-induced, pH-dependent dissociation of casein micelles on heating reconstituted skim milk at temperatures below 100 °C. *Journal of Agricultural and Food Chemistry, 45*(4), 1108–1115.

Anema, S. G., & Li, Y. (2003). Association of denatured whey proteins with casein micelles in heated reconstituted skim milk and its effect on casein micelle size. *Journal of Dairy Research, 70*(1), 73–83.

Beaucage, G. (1996). Small-angle scattering from polymeric mass fractals of arbitrary mass-fractal dimension. *Journal of Applied Crystallography, 29*(2), 134–146.

Dalgleish, D. G., & Corredig, M. (2012). The structure of the casein micelle of milk and its changes during processing. *Annual Review of Food Science and Technology, 3*, 449–467.

Day, L., Raynes, J., Leis, A., Liu, L., & Williams, R. (2017). Probing the internal and external micelle structures of differently sized casein micelles from individual cows milk by dynamic light and small-angle X-ray scattering. *Food Hydrocolloids, 69*, 150–163.

De Kruif, C. G. (1999). Attractive interactions and aggregation in food dispersions. In E. Dickenson, & J. M. R. Patino (Eds.), *Food emulsions and foams; interfaces, interactions and stability* (pp. 29–44). Cambridge, UK: Royal Society of Chemistry.

De Kruif, C. G. (2014). The structure of casein micelles: A review of small-angle scattering data. *Journal of Applied Crystallography, 47*(5), 1479–1489.

Donato, L., & Dalgleish, D. G. (2006). Effect of the pH of heating on the qualitative and quantitative compositions of the sera of reconstituted skim milks and on the mechanisms of formation of soluble aggregates. *Journal of Agricultural and Food Chemistry, 54*(20), 7804–7811.

Donato, L., Guyomarc'h, F., Amiot, S., & Dalgleish, D. (2007). The mechanism of interaction of κ-casein and whey protein in heated milks. *International Dairy Journal, 17*, 1161-1167.

Fejgin, L. A., & Svergun, D. I. (1987). *Structure analysis by small-angle X-ray and neutron scattering*. New York: Plenum Press.

Gonzalez-Jordan, A., Thomar, P., Nicolai, T., & Dittmer, J. (2015). The effect of pH on the structure and phosphate mobility of casein micelles in aqueous solution. *Food Hydrocolloids, 51*, 88–94.

Hansen, S., Bauer, R., Lomholt, S. B., Quist, K. B., Pedersen, J. S., & Mortensen, K. (1996). Structure of casein micelles studied by small-angle neutron scattering. *European Biophysics Journal, 24*(3), 143–147.

He, J.-S., Zhu, S., Mu, T.-H., Yu, Y., Li, J., & Azuma, N. (2011). α_s-casein inhibits the pressure-induced aggregation of β-lactoglobulin through its molecular chaperone-like properties. *Food Hydrocolloids, 25*(6), 1581–1586.

Holt, C., Davies, D. T., & Law, A. J. (1986). Effects of colloidal calcium phosphate content and free calcium ion concentration in the milk serum on the dissociation of bovine casein micelles. *Journal of Dairy Research, 53*(4), 557–572.

Ingham, B., Smialowska, A., Erlangga, G. D., Matia-Merino, L., Kirby, N., Wang, C., … Carr, A. (2016). Revisiting the interpretation of casein micelle SAXS data. *Soft Matter, 12*(33), 6937–6953.

Janhoj, T., Petersen, C. B., Frost, M. B., & Ipsen, R. (2006). Sensory and rheological characterization of low-fat stirred yogurt. *Journal of Texture Studies, 37*, 276–299.

Kethireddipalli, P., Hill, A. R., & Dalgleish, D. G. (2010). Protein interactions in heat-treated milk and effect on rennet coagulation. *International Dairy Journal, 20*(12), 838–843.

Le Graët, Y., & Gaucheron, F. (1999). pH-induced solubilization of minerals from casein micelles: Influence of casein concentration and ionic strength. *Journal of Dairy Research, 66*(2), 215–224.

Li, R., Rovers, T. A. M., Jæger, T. C., Hougaard, A. B., Svensson, B., Simonsen, A. C., & Ipsen, R. (2021). Effect of thawing procedures on the properties of frozen and subsequently thawed casein concentrate. *International Dairy Journal, 112*, Article 104860.

Li, R., Rovers, T. A. M., Jæger, T. C., Wijaya, W., Hougaard, A. B., Simonsen, A. C., … Ipsen, R. (2021). Interaction between added whey protein ingredients and native milk components in non-fat acidified model systems. *International Dairy Journal, 115*, Article 104946.

Liu, D., Yu, Y., Zhang, J., Liu, X., Wang, M., Hemar, Y., … Zhou, P. (2017a). Biochemical and physico-chemical changes of skim milk during acidification with glucono-δ-lactone and hydrogen chloride. *Food Hydrocolloids, 66*, 99–109.

Liu, G., Buldo, P., Greve, M. T., Nielsen, S. B., Nielsen, J. H., & Ipsen, R. (2016). Effects of added whey protein aggregates on textural and microstructural properties of acidified milk model systems. *International Dairy Journal, 62*, 43–52.

Liu, G., Jæger, T. C., Nielsen, S. B., Ray, C. A., & Ipsen, R. (2017b). Interactions in heated milk model systems with different ratios of nanoparticulated whey protein at varying pH. *International Dairy Journal, 74*, 57–62.

Lucey, J. (2002). Formation and physical properties of milk protein gels. *Journal of Dairy Science, 85*(2), 281–294.

Marchin, S., Putaux, J.-L., Pignon, F., & Léonil, J. (2007). Effects of the environmental factors on the casein micelle structure studied by cryo transmission electron microscopy and small-angle x-ray scattering/ultrasmall-angle x-ray scattering. *The Journal of Chemical Physics, 126*(4), 01B617.

Mata, J. P., Udabage, P., & Gilbert, E. P. (2011). Structure of casein micelles in milk protein concentrate powders via small angle X-ray scattering. *Soft Matter, 7*(8), 3837–3843.

Moitzi, C., Menzel, A., Schurtenberger, P., & Stradner, A. (2011). The pH induced sol–gel transition in skim milk revisited. A detailed study using time-resolved light and X-ray scattering experiments. *Langmuir, 27*(6), 2195–2203.

Morgan, P. E., Treweek, T. M., Lindner, R. A., Price, W. E., & Carver, J. A. (2005). Casein proteins as molecular chaperones. *Journal of Agricultural and Food Chemistry, 53*(7), 2670–2683.

Qian, F., Sun, J., Cao, D., Tuo, Y., Jiang, S., & Mu, G. (2017). Experimental and modelling study of the denaturation of milk protein by heat treatment. *Korean Journal for Food Science of Animal Resources, 37*(1), 44.

Tamime, A. Y., Kalab, M., Muir, D. D., & Barrantes, E. (1995). The microstructure of set-style, natural yogurt made by substituting microparticulate whey protein for milk fat. *Journal of the Society of Dairy Technology, 48*, 107–111.

Torres, I. C., Janhøj, T., Mikkelsen, B.Ø., & Ipsen, R. (2011). Effect of microparticulated whey protein with varying content of denatured protein on the rheological and

sensory characteristics of low-fat yoghurt. *International Dairy Journal, 21*(9), 645–655.
Vasbinder, A. J., Alting, A. C., & de Kruif, K. G. (2003). Quantification of heat-induced casein–whey protein interactions in milk and its relation to gelation kinetics. *Colloids and Surfaces B: Biointerfaces, 31*(1–4), 115–123.
Walstra, P., Walstra, P., Wouters, J. T., & Geurts, T. J. (2005). *Dairy science and technology*. CRC Press.
Yang, S., Tyler, A. I. I., Ahrne, L., & Kirkensgaard, J. J. K. (2021). Skimmed milk structural dynamics during high hydrostatic pressure processing from in situ SAXS. *Food Research International, 147*, Article 110527.
Yang, Z., Gu, Q., Banjar, W., Li, N., & Hemar, Y. (2018). In situ study of skim milk structure changes under high hydrostatic pressure using synchrotron SAXS. *Food Hydrocolloids, 77*, 772–776.